Characterization of the Virgo Seismic Environment

Michael W. Coughlin[1, a]

[1] *Carleton College, One North College Street, Northfield, Minnesota 55057;*
Tutor: Irene Fiori, European Gravitational Observatory, Italy

An important consideration for Virgo is to characterize the seismic environment near the detector and understand how environmental effects from the surrounding area couple into the interferometer. During the months of June and July 2010, a Guralp-3TD seismometer was stationed at various locations around the Virgo site. Seismic data were taken and examined, with spectral analysis and coherence with seismometers inside of the detector performed. Environmental effects were noted and attempts were made to identify their sources.

I. INTRODUCTION

The general theory of relativity predicts that all accelerating objects with non-symmetric mass distributions produce gravitational waves (GW). GW presumably should be directly detectable when very massive objects such as black holes or neutron stars undergo acceleration. LIGO (the Laser Interferometer Gravitational-Wave Observatory) [1] and Virgo [2] are some of the detectors searching for GW. These experiments seek to directly detect GW and use them to study astrophysical sources. They seek GW associated with the inspiral of binary neutron stars and black holes and the merger of these, GW burst from supernovae and gamma ray sources, periodic GW from nonaxisymmetric rotating or vibrating neutrons stars, and processes of the early universe which would produce a stochastic background of GW. [1].

Virgo, located in Cascina, Italy, is a laser Michelson interferometer with 3km long, Fabry Perot resonant optical cavities in its arms. With respect to other similar detectors, Virgo has enhanced sensitivity between 10 and 100Hz due to seismic isolation performance of the "super-attenuators" to which the test masses are suspended. Beginning in 2011, the detector expects to undergo upgrades, known as Advanced Virgo (AdV), to improve its sensitivity by one order of magnitude [3]. The Virgo detector is sensitive to a variety of noise sources of non-astrophysical origin, such as instrumental glitches, environmental disturbances, and mechanical resonances. Events not caused by GW in the data often produce significant effects in interferometers, as there is significant power in these signals. These instrumental and environmental artifacts make it difficult to identify a GW unambiguously.

Seismic noise places a limit on Virgo's detection sensitivity. Although Virgo's mirrors are well-isolated from local seismic activity by suspension systems made of multi-stage pendulums, seismic noise remains a concern. One path of seismic noise is that of "diffused light" [4]. Because of unavoidable imperfections in the detector's optical components, some tiny fraction of light can exit the main optical path and strike a surface that is connected to the ground, and thus be subject to the local seismic field. When this light reflects off of mirrors, lenses, or photo-detectors on external optical tables used for detector controls, it is often diffused over a wide solid angle and a fraction of it can re-enter the main beam path but with a slightly different phase (as it took a longer path). This phenomena functions as extra noise in the GW channel and limits its sensitivity.

Because seismic events couple in this way into the GW channel, it is necessary to understand and mitigate the noise from the local seismic environment. To assist in this effort, the Virgo detector is supplemented with several environmental sensors, including seismometers and accelerometers, that monitor the local environment [5]. These channels are used to detect environmental disturbances that can couple to the GW channel and are strategically placed in sensitive areas of the interferometer. To reduce the influence of anthropogenic noise, during the Advanced Virgo upgrade, machines that are identified as seismically and acoustically affecting the interferometer will be replaced, moved, or isolated [3]. The current proposal is to move all chillers, water pumps, air compressors, and air conditioners from their current locations to some defined distance from the interferometer. By placing these machines on their own foundations as well as adopting techniques to reduce noise emission and propogation, Virgo hopes to significantly reduce their affect on the detector. To prioritize projects to reduce noise at Virgo, a careful documentation of the present local seismic environment is necessary, as well as identification among the infrastructure machines of relevant sources of seismic noise reaching the detector's sensitive components. The work described hereafter is part of this effort.

[a] Electronic address: coughlim@carleton.edu

Section Letter	Building Name	Location in Building	Location Compared To	Distance Between Seismometers (meters)
A	Technical Building One	Ground Floor	Central Building: Ground Floor	80
B	Building One	First Floor	Central Building: Ground Floor	105
C	Outside Building One	Ground Floor	Mode Cleaner: Ground Floor	30
D	Outside Mode Cleaner Building	Ground Floor	Mode Cleaner: Ground Floor	10
E/F	West/North End Building	Ground Floor	West/North End Building: External Optical Bench	20

TABLE I: Locations of seismometer placement.

Building Name	Known Machinery near Seismometer
Technical Building One	Water Boiler and Pumps, Air Compressor (Ground Floor); Air Handler Unit, Cold Water Pumps, Air Compressor (First Floor); Cold Water Chiller (1 and 2)
Building One	Computer Air Conditioners (First Floor); Building One Air Conditioners (Roof)
Outside Building One	Two Air Conditioners
Outside Mode Cleaner Building	Cold Water Chiller and Pumps
West/North End Building	Cold Water Chiller, Water Boiler, Generator Set, UPS machines, Main Boards, Transformer, Air Compressor, Water Pumps, Air Handler Unit

TABLE II: Information about machinery in measurement locations.

During the months of June and July 2010, a Guralp-3TD seismometer was stationed to monitor floor vibrations at various technical areas around the Virgo site which host several infrastructure machines (i.e. water chillers, heaters, pumps). Seismic data were first examined with spectral analysis, and several single sources are identified using correlation of the seismic data with synchronous records of the infrastructure machines working status (i.e. temperature monitors, voltage sniffers). Then, seismic data were correlated with the synchronous record of permanent seismic probes close to the detector. Coherence and spectral ratio techniques are used to select "relevant" sources whose noise emissions reach the detector and measure the noise attenuation between the sources and detector. Note that for designing AdV noise mitigation, it is important to get an idea of the seismic attenuation that can be achieved by moving sources at a given distance from their present location. Measured noise reduction factors are finally analyzed to this end.

Section 2 discusses the methods used when taking and analyzing data. Section 3 characterizes the noise emissions from the sources found in this analysis at the various locations, while Section 4 provides an estimate for the attenuation of the noise spectral peaks as a function of distance. Appendix A includes maps of the locations studied, while Appendix B provides tables containing information about lines found. Finally, Appendix C provides power spectral density and coherence plots for all of the locations studied.

II. CHARACTERIZATION METHODS

A. Measurement Setup

Using a Guralp-3TD tri-axial velocimeter, specifications for which can be found here [6], data were taken at six locations around the site using a sampling rate of 250Hz. The Guralp seismometer is equipped with a GPS antenna receiver to synchronize its data to Virgo seismic channels. Maps for the site and the locations of the measurements can be seen in Figure 1. These locations were chosen for their proximity to machinery known to create large seismic noise. These locations are detailed in Table I, with the machines at each location in Table II and maps included in Appendix A. In each location, the Guralp seismometer was installed on the same concrete platform where the machinery sit and if possible, at a distance of at least a few meters from the machinery to prevent saturation. For each location, the Power Spectral Density (PSD) of the Guralp seismometer, called also the "test probe," is computed, an example for which can be seen in Figure 2. Each measurement lasts approximately 24 hours in order to determine the hourly and daily cycle operation for the machines. This measurement is compared with a tri-axial seismometer, called also the "reference probe," permanently stationed in the closest nearby experimental area containing sensitive interferometer components [5]. In the Mode Cleaner, West End, and North End Buildings, the reference probe was a Episensor FBA ES-T, while in the Central Building, the probe was a Guralp CNG-T40. To identify the characteristic frequencies for some machines, a PCB accelerometer, specifications for which can be found here [7], was used in conjunction with a spectrum analyzer.

B. Analysis Methods

Important noise components are frequency lines (persistent spectral peaks) that appear as significantly coherent (coherence rising out of the background) between the test and reference probes, which establishes the cause of the line being the same in both seismometers. Coherence itself does not allow one to disentangle seismic signals generated

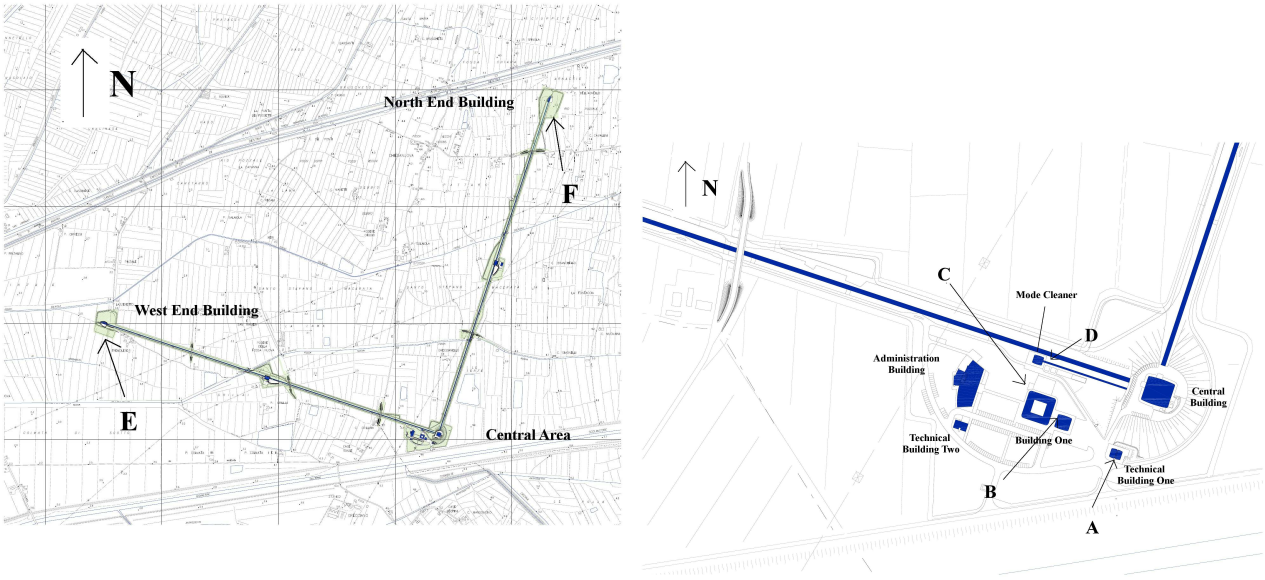

FIG. 1: Left: Arial View of the Virgo Interferometer. Right: Arial view of Virgo's Central Area. Measurement sites are marked with the letter (corresponding to those given in Table I).

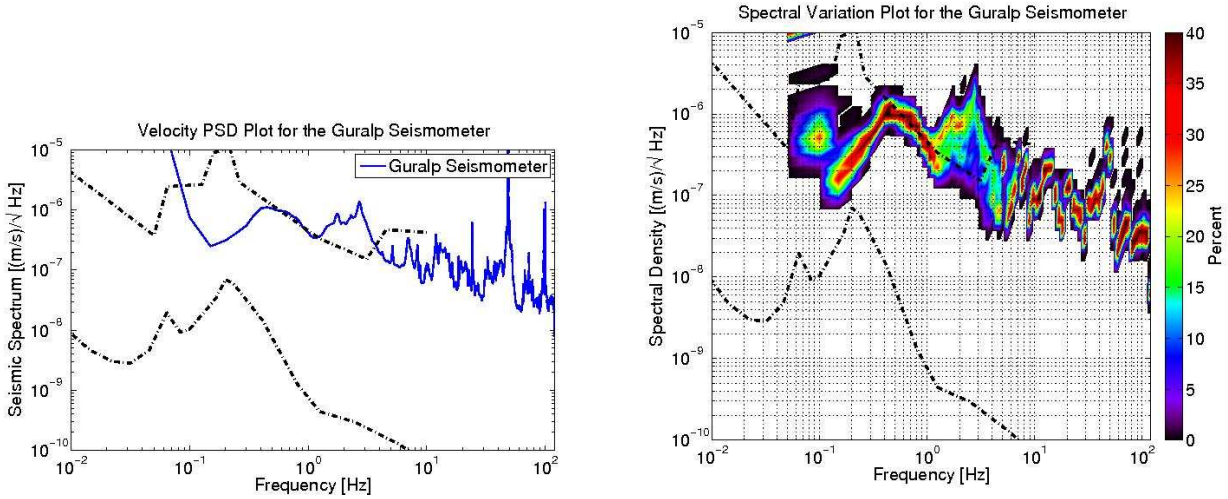

FIG. 2: Left: Averaged root spectral density of the modulus of the the components of the Guralp seismometer at the Virgo site during a day in June of 2010. The two dashed curves correspond to the Peterson low- and high-noise models [8]. Right: Variation in the root spectral density of the seismometer on that same day.

close to the test probe (i.e. machinery under test) or to the reference probe (i.e. cooling fans of electronic units). In order to determine when the former is the case, the ratio of the PSDs of "test" to "reference" seismometers is examined, and coherent lines are selected which have a positive spectral ratio. PSDs and coherence plots can be seen in Appendix C. Water pumps and cooling fans are some examples of machines giving off continuous lines. If the source is not obvious, suspected machines are analyzed with the PCB accelerometer and spectrum analyzer, comparing the machines' characteristic frequencies to those seen in the coherence. These lines are detailed in tables in Appendix B of the paper.

Periodic lines, on the other hand, are more difficult to identify. Because the lines come and go, they tend to be washed out in PSD averaging. For this reason, Time-Frequency plots of the PSDs are produced and examined by eye for periodic lines. In order to identify the source of these lines, the periodic line must be first quantified in some way. To study the average amplitude of the seismic signal in a frequency band, one can compute the root-mean-square

(RMS) in that band, which is defined as:

$$RMS = \sqrt{\sum_{i=1}^{n} {x_i}^2 * \delta f} \tag{2.1}$$

where x_i is the ith component of the frequency band in question and δf is the width of the frequency bins in the spectrum. The sum goes from i=f_1 to i=f_2, where f_1 and f_2 are the minimum and maximum frequencies respectively in the frequency band. This RMS value can then be compared to the time series of various Infrastructure Machine Monitoring System (IMMS) signals, including temperature and pressure probes, to identify their source. All periodic lines found are studied as their effect on the interferometer is more difficult to quantify (due to averaging, proximity to continuous lines, etc.). In the following section, results of these methods are presented for each data record.

In an attempt to quantify the noise mitigated by the distance of the machinery from experimental areas, the ratio of the PSDs of both probes for the identified lines was measured. In this way, an approximate estimate of the attenuation factor as a function of distance was measured and presented in Section 4.

III. CHARACTERIZATION RESULTS

A. Characterization of Noise from Technical Building One

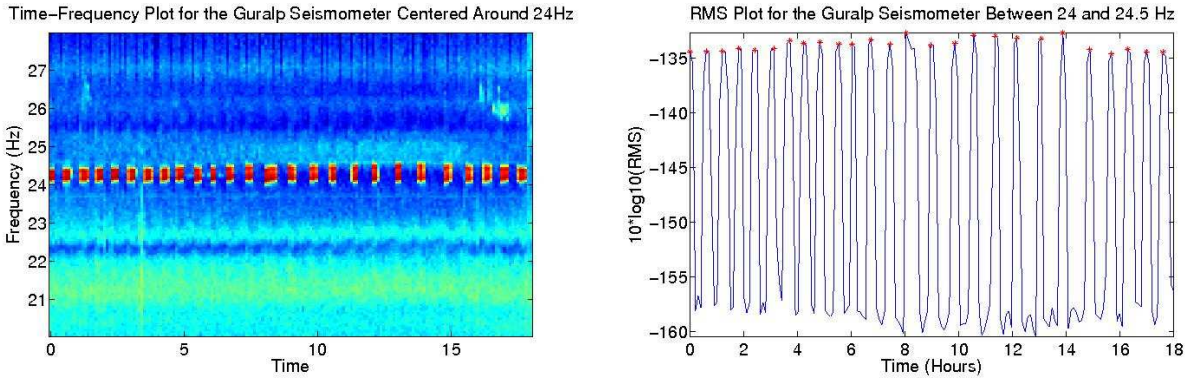

FIG. 3: Left: PSD as a function of time and frequency of the Guralp seismometer in TB1 zoomed in on the 24 Hz region. Right: A plot of the RMS around the periodic line at 24.2Hz of the Guralp seismometer. The red stars correspond to peaks found in the RMS, which provided an estimate of the period and frequency of the line.

The first data were taken in Technical Building One (TB1) and compared with data from a seismometer on the floor of the Central Building (CB), where the two arms of the interferometer converge, and GW detection occurs. These two probes are approximately 80 meters apart. Figures 18 and 19 (Appendix A) show the location of the test and reference seismometers and of machinery in TB1. The PSDs of the test and reference probes, as well as the coherence between them, can be seen in Figure 22. These noise lines are documented in Table III. A structure around 24Hz is seen, which is showed in detail on the left of Figure 3. The periodic line, which is at 24.2 Hz with harmonics at 48.4 and 72.6 Hz, was studied closely. The frequency band of the RMS in this case is f_1=24Hz and f_2=24.5Hz, a plot for which can be seen on the right of Figure 3. From this plot, the line's period is estimated at about 42 minutes.

In order to determine the importance of this periodic noise line, it was necessary to find out if this line was appearing in the CB. To do so, the spectrum of the seismometer permanently stationed in the CB was examined, which can be seen on the left of Figure 5. A clear periodic line around 24.2Hz can be seen in the spectrum, similar to that of the seismometer in TB1. In order to find the source of the periodic line, it was necessary to determine in which building the line was louder. The ratio of the PSDs around 24.2 Hz (Seismometer in TB1/Seismometer in CB) was approximately 16, shown in Figure 4, indicating the source of the line to be in TB1. The coherence around this line was about 0.6, indicating a strong correlation between the two seismometers at that frequency.

The time series of a number of monitors of the machinery in TB1 were compared with the RMS of the 24.2Hz signal in the Guralp seismometer, one of which may be seen on the right of Figure 5. From this figure, the RMS in the 24Hz band of the Guralp seismometer is clearly correlated with time series of a temperature monitor of the first water

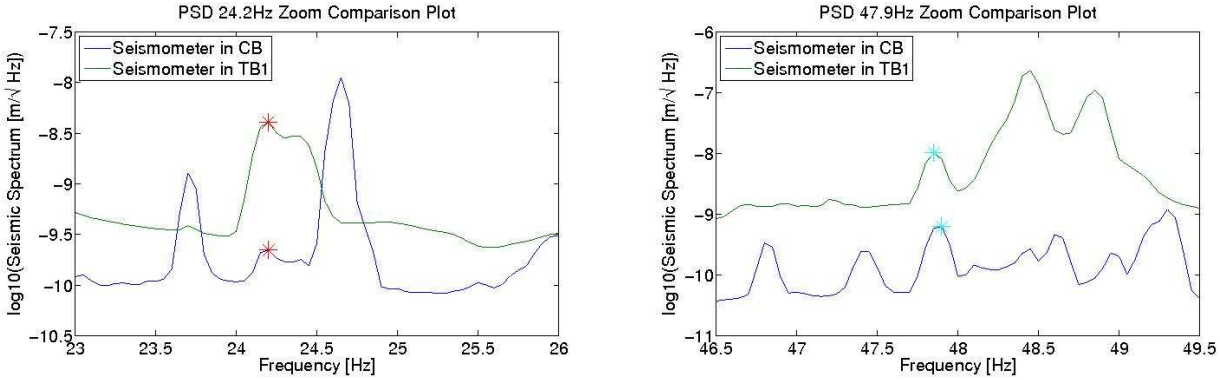

FIG. 4: Left: PSDs of the seismometers in TB1 and the CB around the 24.2Hz periodic line. The peak to the left of the 24.2Hz line is known to be the CB's DAQ room air conditioning unit, while the peak to the right is the scroll pump, which is turned off during science mode. Right: PSDs of the seismometers in TB1 and the CB around the 47.9Hz continuous line.

chiller. One can see that when the temperature of the water reaches a high point, the cold water chiller switches on, causing the temperature of the water to decrease. When the temperature reaches a low point, the water chiller switches off and the whole process starts again. The chiller is located on the roof of TB1, as can be seen on the left of Figure 19. It is provided with insulating springs, although it is possible that the vibrations can travel through the rigid water pipes between TB1 and the CB or in the water itself. Better insulation for these parts, such as flex joints, will be studied.

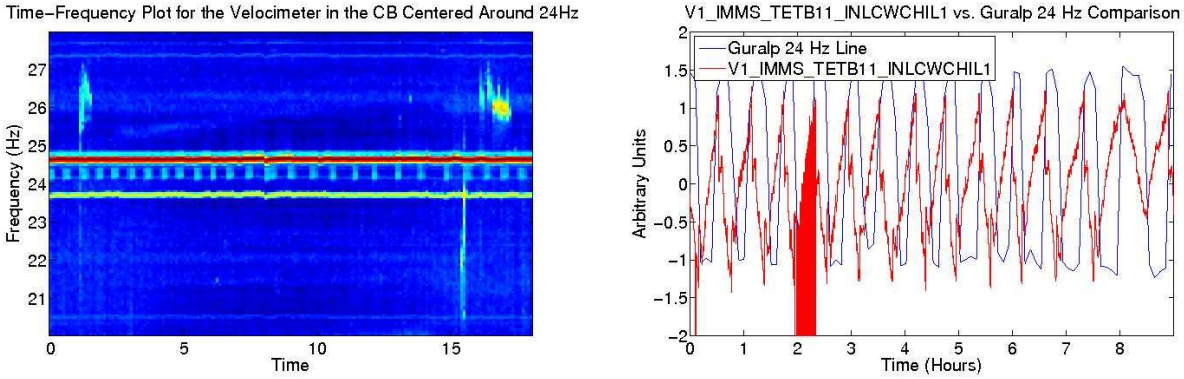

FIG. 5: Left: This plot shows the PSD as a function of time and frequency around 24Hz in the modulus of the three components of the seismometer in the CB. Right: A plot of both the RMS in the 24Hz band of the Guralp seismometer as well as the time series of a temperature monitor of the first (of two) cold water chillers.

B. Characterization of Noise from Building One

The second data were taken in Virgo's Building One (B1) and compared with the same seismometer in the CB. These two probes are approximately 105 meters apart. Figure 19 (right) in Appendix A shows the location of the test seismometer and analyzed machinery on B1's roof. The PSDs of the test and reference probes, as well as their coherence, can be seen in Figure 23. The noise lines are documented in Table IV. It was suspected that the lines seen in the coherence originated in either the computer fans on the first floor of B1 or the air conditioning units on the roof of B1. In order to check this hypothesis, the characteristic mechanical frequencies of these machinery were examined with the PCB accelerometer, which can be seen in Figure 6.

Two of the lines found in the machinery, 19.3Hz and 48.4Hz, match up well with two coherent lines documented in Table IV. Shown in Figure 7 are the comparative strengths of these lines measured close to the machinery and 105 meters away inside the CB. The strenghth of both lines is significantly above the background in the CB, which makes these lines interesting. While the source of the noise lines measured by the Guralp test probe is most likely the B1 computer fans, the association to noise lines in CB is not certain, for the reasons discussed below. Concerning the

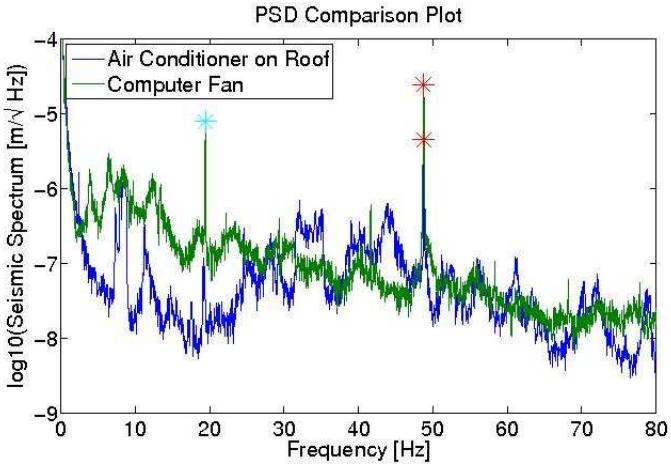

FIG. 6: This plot shows the PSD for both a fan in the computer room as well as an air conditioner on the roof. The data were taken with a portable probe in direct contact with the machines under study. Both show strong lines around 48.4Hz, which are shown by the red stars on the right, and the computer fan shows a strong line around 19.3Hz as well, which is shown by the blue star on the left.

48.8Hz line, it is important to note that many Virgo motors are "squirrel double-cage AC Asynchronous Induction Motors," which are common medium-size motors. These motors usually run at half the speed of the frequency of the power main, which in Europe is 50Hz, while smaller motors run at approximately the same speed as the power main. Thus the larger motors run at approximately 25Hz, but due to friction effects, the real rotating frequency is slightly less than this. For this reason, values span around 24Hz for larger (double cage) motors and 48Hz for smaller (single cage) motors. Thus, lines seen near these frequencies can come from multiple sources, including smaller motors and water pumps also located inside the CB much closer to the detector, and so it is more difficult to exactly identify their source. In a previous switch off test of an air conditioning unit in the DAQ room in the CB (described in elog entry 24621), one line around 19.4Hz was noted. As machine lines tend to wander, it is possible that the lines seen in the CB are caused by this machine instead.

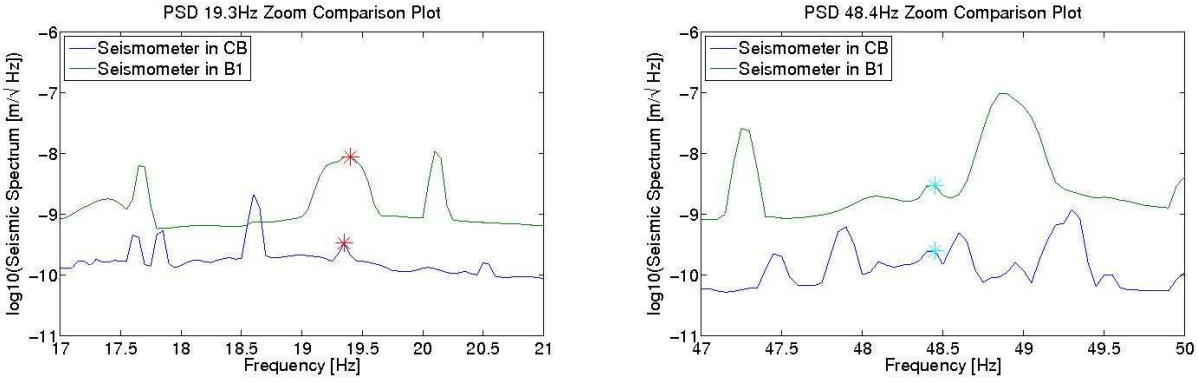

FIG. 7: Left: PSDs of the seismometers in B1 and the CB around the 19.3Hz continuous line. Right: PSDs of the seismometers in TB1 and the CB around the 48.4Hz continuous line.

C. Characterization of Noise from Chillers Outside Building One

The third data were taken on a platform between B1 and the Mode Cleaner Building (MC) and compared with a seismometer in the MC (map in left of Figure 20, in Appendix A). The MC contains the end mirror of the Input Mode Cleaner optical cavity and filters jitter and power noise as well as higher order modes from the beam. The distance between these probes is approximately 30 meters. On this platform resides two chillers, a small one which serves the Seminar Room (SR) in B1 and a larger one which serves the rest of B1. The PSDs of the test and reference probes,

as well as their coherence, can be seen in Figure 24. These noise lines are documented in Table V.

There are no IMMS probes monitoring the processes of these machines, and thus for indentification of periodic lines, information from Virgo personnel is relied on. In order to find the source of the significant noise lines, vibration noise of both chillers was measured using the spectrum analyzer and the portable accelerometer. It is known that the SR chiller is on continuously during the day (from 9 A.M. to 6 P.M.) and turns on during the night when the SR falls below a certain temperature. Similarly, the B1 chiller is only on during the day and not during the night. This effect can be seen in Figure 9, where a line at 60Hz can be seen on continuously during the main working hours (0-6 Hours on the plot) and only periodically during the night, showing that it corresponds to the SR chiller. On the other hand, a broadband line around 90Hz can be seen on during only working hours, thus corresponding to the B1 chiller. Upon comparison with the coherence results, a number of the low frequency lines were identified, the most relevant two from the chillers at 15.6Hz and 21.8 Hz are shown in Figure 8. Higher frequency lines (58.7Hz and 87.3Hz) are emitted from the sources but their coherence with the reference probe at the MC floor is negligible, possibly because their amplitude falls below the local seismic background in the MC generated by sources inside the building (i.e HVAC machine, electronic racks).

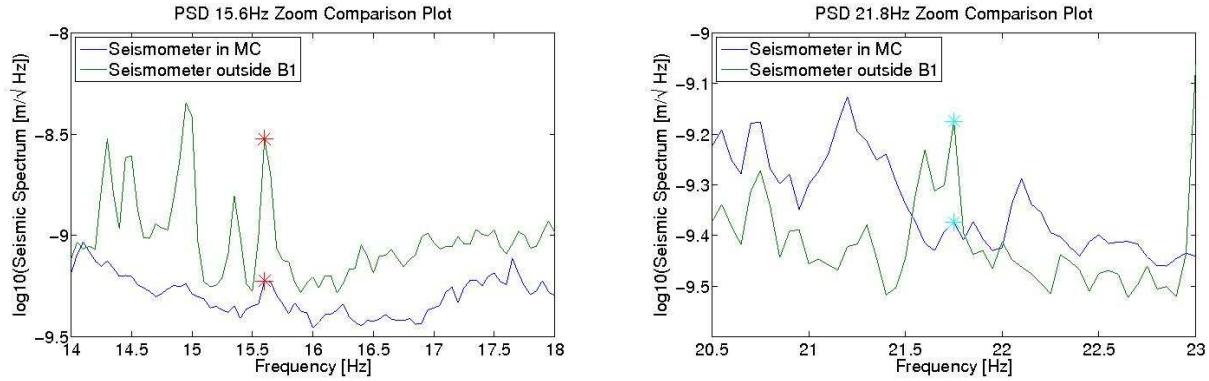

FIG. 8: Left: PSDs of the seismometers outside B1 and in the MC around the 15.6Hz continuous line. Right: PSDs of the seismometers outside B1 and in the MC around the 21.8Hz continuous line.

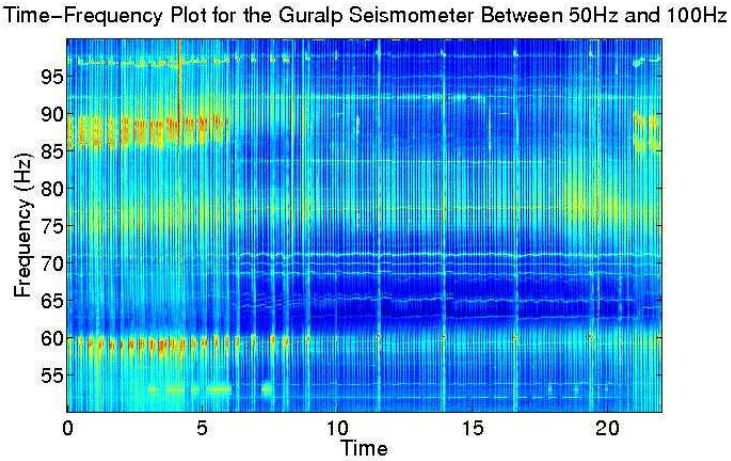

FIG. 9: This plot shows the Time-Frequency plot for the Guralp seismometer placed near the chillers of B1 between 50Hz and 100Hz.

D. Characterization of Noise from the Cold Water Chiller Outside the Mode Cleaner

The fourth data were taken outside the MC, on the same concrete platform as the MC's cold water chiller, and compared with the seismometer inside of the MC. The distance between these probes is approximately 10 meters (see

map in left of Figure 20, in Appendix A). The PSDs of the test and reference probes, as well as the coherence, can be seen in Figure 25. These noise lines are documented in Table VI.

In viewing the PSD plots, a number of significant lines are noticed. This includes continuous lines at 24.2Hz and 38.8Hz, which can be seen on the left of Figure 10. A strong periodic line at 48.9Hz, which has a harmonic at 97.8Hz, can be seen on the right of Figure 10. To study this line, the RMS around the 48.9Hz band was computed and compared to probes inside of the MC. A water temperature probe follows this line well, as can be seen in Figure 11, indicating its source is the MC water chiller. This line is important since coherence was noted at its frequency between the GW channel of VSR2 run data and the seismometer in the MC. Thus, it seems that the MC water chiller affects the Virgo sensitivity and for this reason, requires prompt attention for noise reduction.

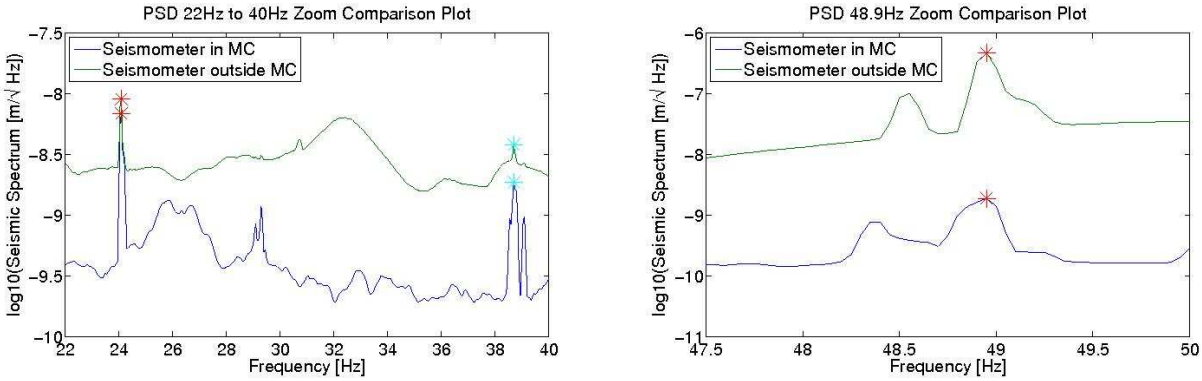

FIG. 10: Left: PSDs of the seismometers outside the MC and in the MC between 22Hz and 40Hz. The red stars on the left correspond to the 24.2Hz continuous line while the blue stars on the right correspond to the 38.8Hz continuous line. Right: PSDs of the seismometers outside the MC and in the MC around the 48.9Hz periodic line.

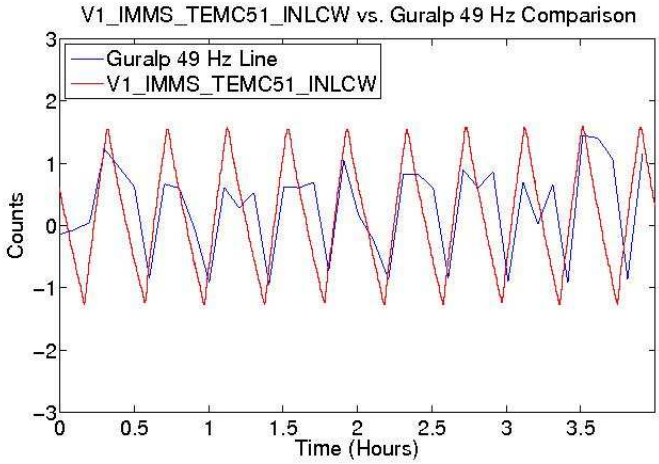

FIG. 11: A plot of both the RMS in the 48.9Hz band of the Guralp seismometer as well as the time series of a temperature monitor of the water chiller.

E. Characterization of Noise in the West End Building

The fifth data were taken inside the West End Building (WEB) near the machinery and compared with a Episensor seismometer located on the external optical bench. The distance between these probes is approximately 20 meters (map in Figure 21, in Appendix A). The PSDs of the test and reference probes, as well as the coherence, can be seen in Figure 26. These noise lines are documented in Table VII.

Upon viewing the PSD plots, a number of significant lines are noticed, including continuous lines at 24.7Hz, 47.1Hz, and 48.8Hz, which can be seen in Figure 12. Using the PCB accelerometer, the 48.8Hz line was identified as coming from the cold water pump in the WEB. Similarly, the 47.1Hz line was attributed to the warm water pump. Due to the

low attenuation of this line between the machinery and experimental area, it is thought that there is a pipe running between the two areas, and this will be investigated further. A number of the lines seen can also be attributed to the air conditioning unit in the WEB. Periodic lines at 22.1Hz and 14.9Hz are also present in the PSD of the test probe. To study these lines, the RMS around both of these bands was computed and compared to probes inside of the WEB. The 22.1Hz line, which has a period of about 49.6 minutes, follows approximately the temperature probe of a cold water chiller, as can be seen in Figure 14, although it has approximately half the period of the probe. The 14.9 Hz line has a period of approximately 25.7 minutes, but this did not quite follow any of the sensors exactly. Lines at 24.7Hz, 47.1Hz, and 48.8Hz are most interesting since reach the external optical bench with large intensity. The 24.7 Hz still lacks identification. The 47.1Hz and 48.8 Hz are associated to the "warm" and "cold" water pumps respectively as verified with the PCB probe in Figure 13. The 47.1 Hz signal reached the bench with almost no attenuation. It is possible that a preferred path, for example through water pipes, exists, which has to be investigated further.

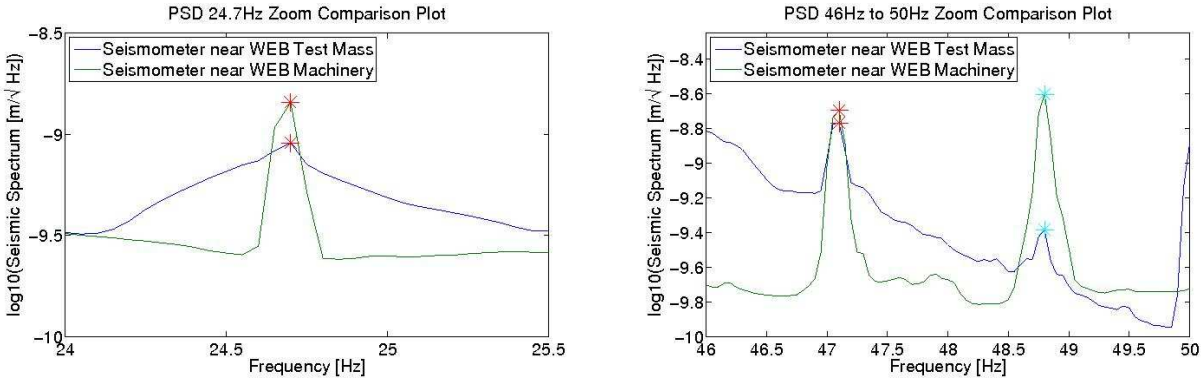

FIG. 12: Left: PSDs of the seismometers near the WEB Machinery and the WEB test mass around the 24.7Hz continuous line. Right: PSDs of the seismometers near the WEB Machinery and the WEB test mass between 46Hz and 50Hz. The red stars on the left correspond to the 47.1Hz continuous line while the blue stars on the right correspond to the 48.8Hz continuous line.

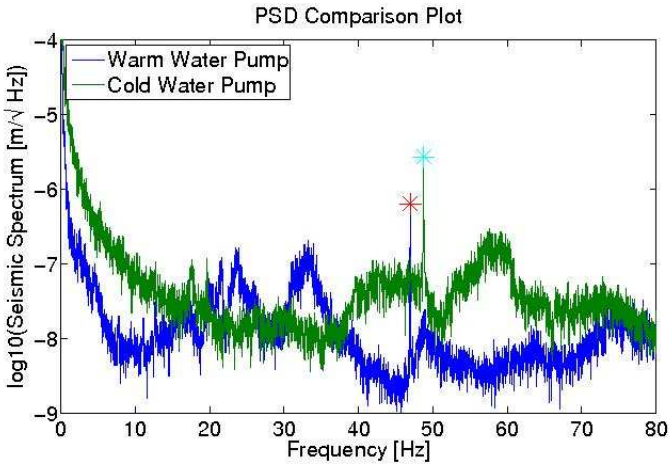

FIG. 13: This plot shows the PSD for both the warm and cold water pumps in the WEB. The data were taken with a portable probe in direct contact with the machines under study. The warm water pumps shows a strong line around 47.1Hz, which is shown by the red star on the right. The cold water pump shows a strong line around 48.8Hz, which is shown by the blue star on the left.

F. Characterization of Noise in the North End Building

The sixth data were taken inside the North End Building (NEB) and compared with a seismometer located on the external optical bench. The distance between these probes is approximately 20 meters. The PSDs of the test and reference probes, as well as the coherence, can be seen in Figure 27. These noise lines are documented in Table VIII.

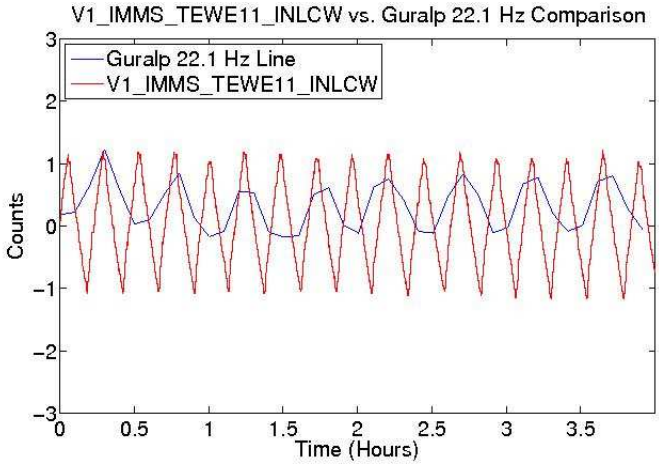

FIG. 14: A plot of both the RMS in the 22.1Hz band of the Guralp seismometer as well as the time series of a temperature monitor of a cold water chiller.

Upon viewing the PSD plots, a number of significant lines are noticed, including continuous lines at 22.8Hz and 48.7Hz, which has a harmonic at 97.4Hz, which can be seen in Figure 15. A number of the lines can be attributed to the air conditioning unit in the NEB, as they were identified in a previous switch off test. Similarly, periodic lines at 48.2Hz and 58.8Hz, which has a harmonic at 117.6Hz, are present in the PSD of the test probe. The RMS around both of these bands was computed and compared to probes. The 48.2Hz line, which has a period of about 108 minutes, follows approximately the temperature probe of a water heater, as can be seen in Figure 16. The 58.8Hz line has a period of approximately 18.3 minutes, but this did not quite follow any of the sensors exactly.

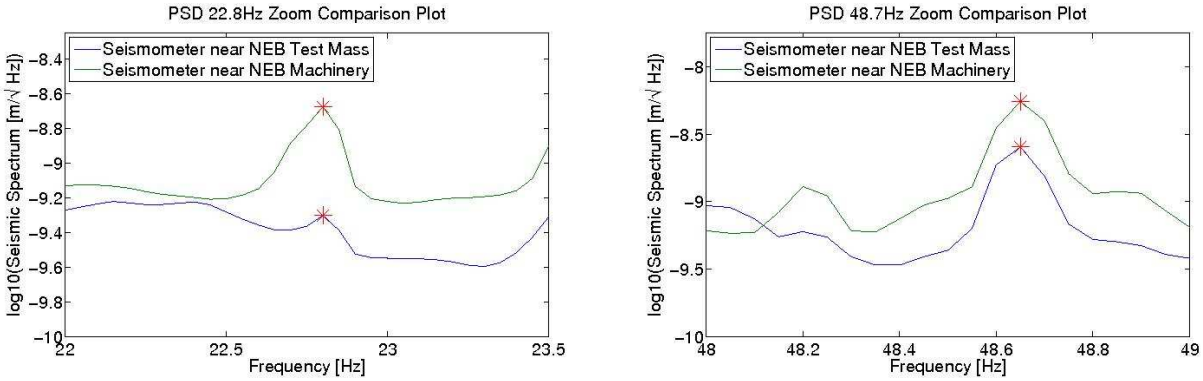

FIG. 15: Left: PSDs of the seismometers near the NEB Machinery and the NEB test mass around the 22.8Hz continuous line. Right: PSDs of the seismometers near the NEB Machinery and the NEB test mass around the 48.7Hz continuous line.

IV. ATTENUATION MEASUREMENT

One of the goals of this project was to attempt to measure how much noise reduction occurs when a machine is on its own foundation and a certain distance away from an experimental area. To measure this attenuation, the PSD ratio of the lines at the different locations were plotted as a function of distance between the probes, the result for which can be seen in Figure 17. A simple model for the dissipation of seismic energy radiated along circular wave fronts from a point-like source is $1/sqrt(r)$, where r is the distance from the point source. Eventually, an exponential factor applies which accounts for the absorption of seismic energy in an homogeneous medium like soil. This has the form exp $\frac{-\pi r f_0}{Qv}$ where f_0 = wave frequency, v = wave speed, and Q = soil absorption factor.

As can be seen in the plot, distances of less than 40 meters have an attenuation of approximately a factor of 3, while distances of about 80 meters and greater have values greater than 10. Indeed, the simple noise attenuation model does not apply in most of the examined cases. One reason is that point-like source approximation is not correct at very

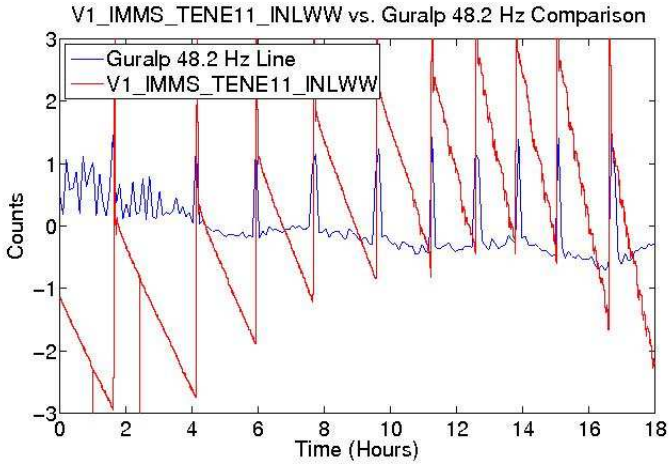

FIG. 16: A plot of both the RMS in the 48.2Hz band of the Guralp seismometer as well as the time series of a temperature monitor of a warm water chiller.

short distances, as for near-field waves, local reinforcement can occur. Reinforcements can be also due to mechanical resonances of the two platforms (technical area and experimental area) which are excited by the seismic emissions. Another important reason is that in most cases, propagation does not uniquely occur through soil. Preferred (less dissipative) paths can exist, such as through water pipes or pressure waves inside the water itself. This is the case for several examined water chillers, heaters, and pumps. Exceptions are the B1 vs. CB ("section B") and the B1 vs. MC ("section C"), for which no rigid pipes connections exist between the machinery and the experimental area. In the former case (B1 vs. CB), because of the large distance (105 meters), the point-like model might reasonably be applied. Indeed, the measured attenuation (lower limit) agrees better with the model expectation.

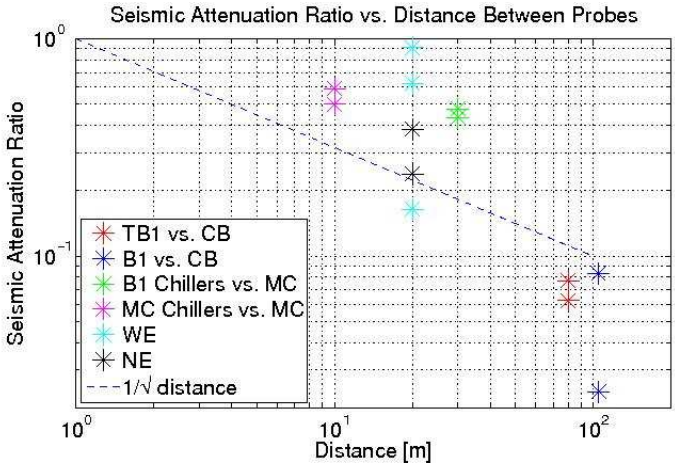

FIG. 17: A plot of the average of the PSD ratio of the coherent lines found in each location as a function of distance between the probes. For the attenuation factors from a distance of 105 meters, the given values are lower limits.

V. CONCLUSION

Noise from several Virgo infrastructure devices, such as water chillers, heaters, and pumps, seismically affects sensitive parts of the interferometer. Although an impact on the present interferometer is not evident in Virgo's sensitivity (with the exception of the MC chiller), the noise reaching the experimental area is, in several cases, considerably above the background, and a noise reduction will be necessary for AdV.

From the present study, we conclude that by only displacing machinery at a pratical distance of 10 to 20 meters from their present positions would not sufficiently reduce their impact. On the other hand, noise transmission through

soil can be more efficiently reduced by the use of seismic isolation systems (i.e. springs). A preferred path through pipes or pressure waves in the fluid is suspected. This needs further investigation in order to plan effective mitigation actions.

Further beneficial studies might include setting up a noise source with known power and characteristic frequencies on its own foundation at various distances from a sensitive experimental area. This would allow for a comprehensive study of the amount of noise reduced as a function of distance, something this study was limited in.

Acknowledgments

This project is funded by the NSF through the University of Florida's IREU program. The work has been carried on also thanks to the support coming from Italian Ministero dell'Istruzione, dell'Universita' e della Ricerca through grant PRIN 2007NXMBHP.

---

[1] B. Abbott et al. LIGO: The Laser Interferometer Gravitational-Wave Observatory. *Reports on Progress in Physics*, 72, 2009.
[2] F. Acernese et al. Status of Virgo. *Classical and Quantum Gravity*, 25, 2008.
[3] F. Acernese et al. Advanced Virgo Preliminary Design. *Virgo Internal report: VIR-0089A-08*, 2008.
[4] T. Accadia et al. Noise from scattered light in virgos second science run data. *Submitted to GWDAW14 proceedings*, 2010.
[5] F. Barone, F. Garufi, and L. Milano. Environment monitoring parameters. *VIRGO Document VIR-MAN-NAP-5800-102*, 2001.
[6] V. Boschi and A. Gennai. Gralp cmg-3td and cmg-eam quick guide. *VIRGO Document VIR-0172A-10*, 2010.
[7] Piezotronics. Accelerometer model 393b12 specification sheet. *Piezotronics Document*, 2010.
[8] Jon Peterson. Observations and modelling of background seismic noise. *Open-file report*, 1993.

APPENDIX A: BUILDING MAPS

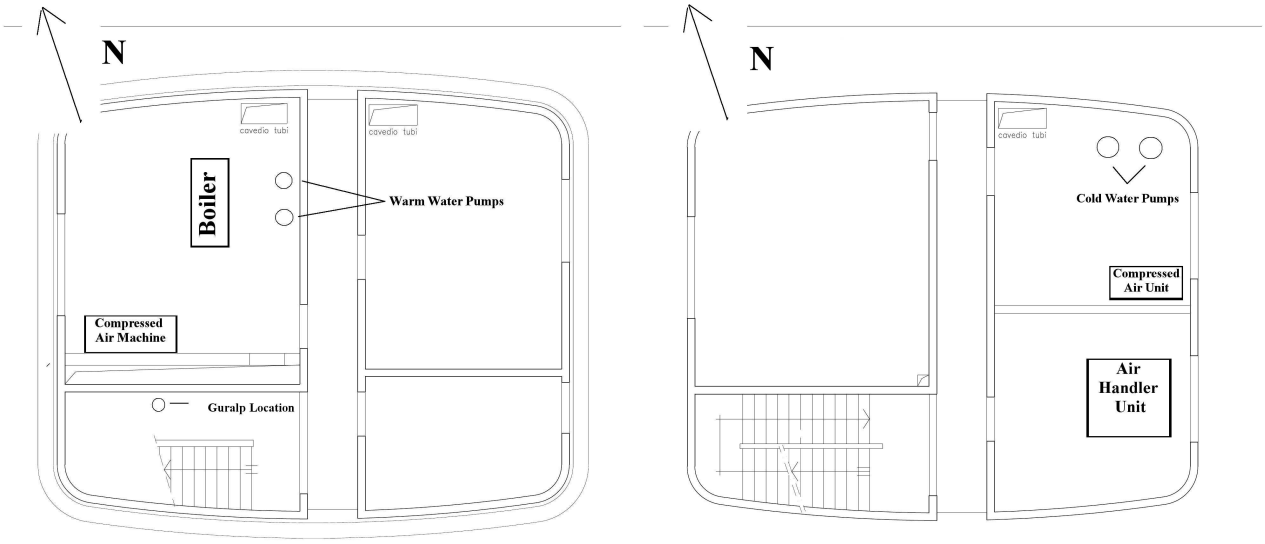

FIG. 18: Left: Map of the ground floor of Technical Building One. Right: Map of the first floor of Technical Building One.

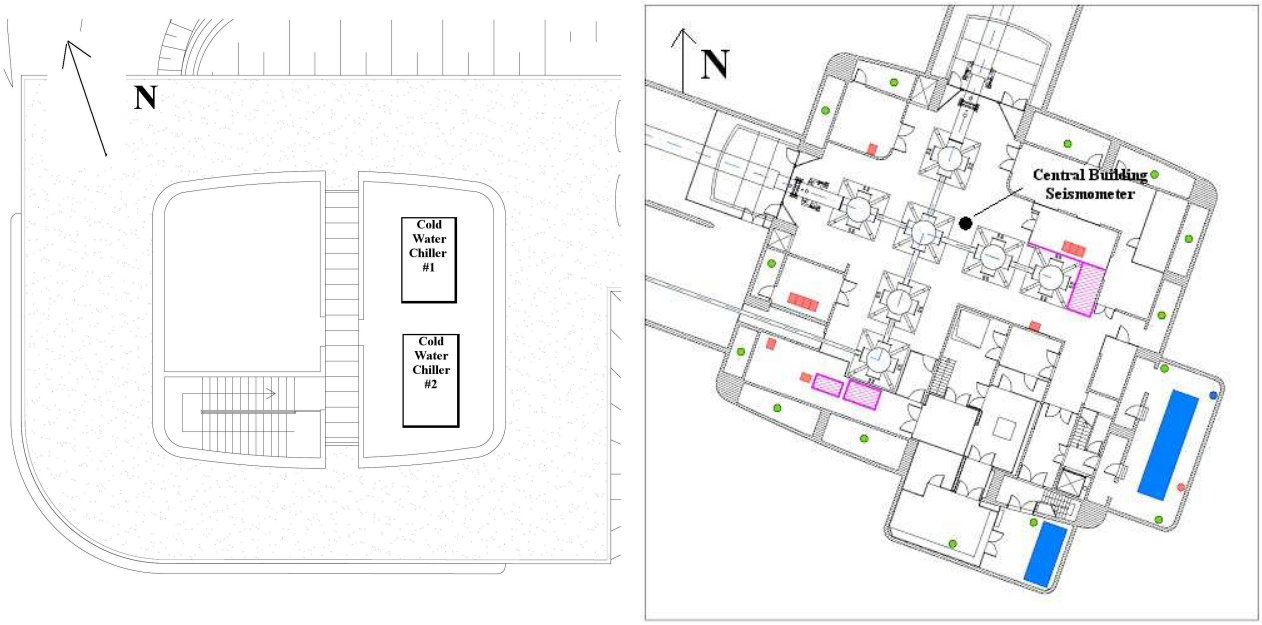

FIG. 19: Left: Map of the roof of Technical Building One. Right: Map of the ground floor of the Central Building.

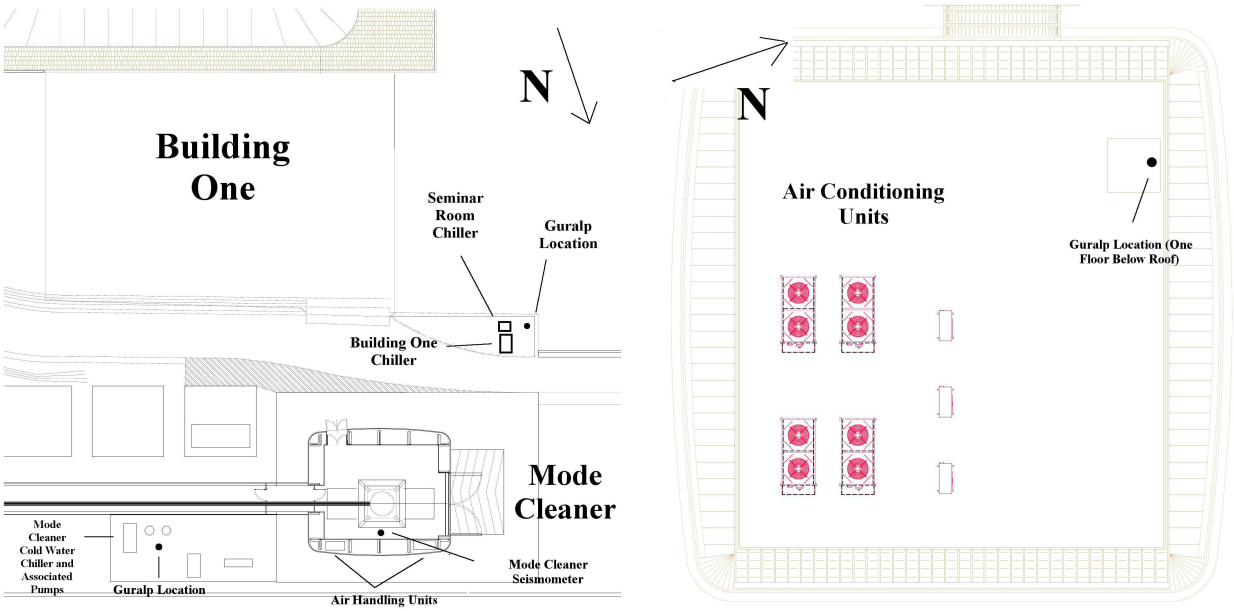

FIG. 20: Left: Map of both Building One and the Mode Cleaner. Right: Map of the roof of Building One.

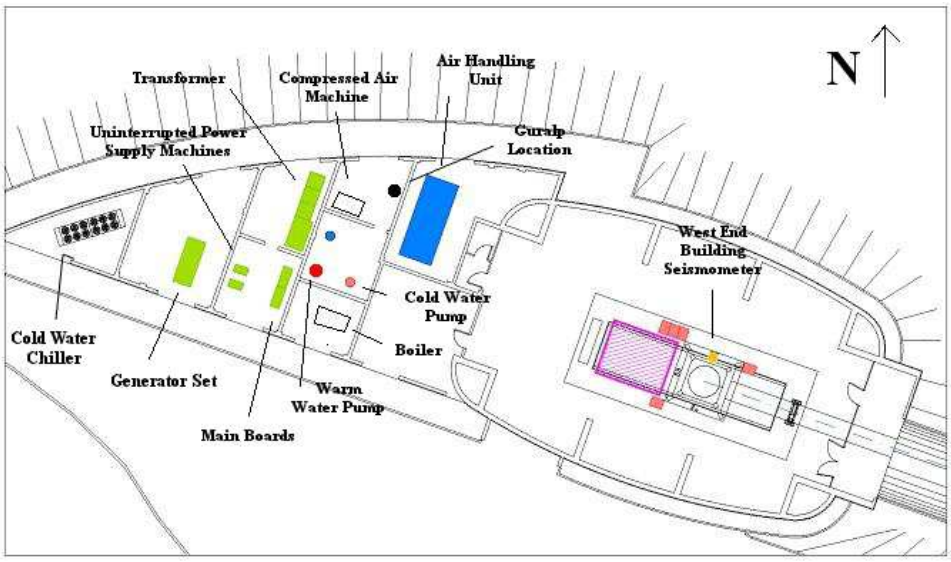

FIG. 21: Map of the West End Building.

Frequency (Hz)	Periodicity (Period)	Suspected Source	Coherence	PSD in TB1	PSD in CB	PSD Ratio (Test/Reference)
24.2, 48.4,78.6	Periodic (42 Minutes)	Cold Water Chiller 1	0.60	$2.73 * 10^{-9}$	$1.70 * 10^{-10}$	16
47.9	Continuous	Water Pump	0.26	$8.12 * 10^{-9}$	$6.27 * 10^{-10}$	13
65	Periodic (19 Minutes)	Unknown	Negligible	$9.05 * 10^{-11}$	$5.01 * 10^{-11}$	2
67	Periodic (33 Minutes)	Unknown	Negligible	$1.58 * 10^{-10}$	$6.09 * 10^{-11}$	3

TABLE III: Noise lines found in PSD of seismometer in TB1. The table provides the line's frequency, periodicity, suspected source, coherence with a seismometer stationed in the CB, the average PSD of the line in TB1, the average PSD of the line in the CB, and the ratio of those PSDs.

Frequency (Hz)	Periodicity (Period)	Suspected Source	Coherence	PSD in B1	PSD in CB	PSD Ratio (Test/Reference)
19.3	Continuous	Computer Fans	0.22	$6.99 * 10^{-9}$	$1.69 * 10^{-10}$	42
48.4	Continuous	Computer Fans and Air Conditioners	0.63	$2.89 * 10^{-9}$	$2.39 * 10^{-10}$	> 12

TABLE IV: Noise lines found in coherence between B1 and CB. Note: As frequencies around 48Hz can come from a number of sources, we quote the ratio as an upper limit.

Frequency (Hz)	Periodicity (Period)	Suspected Source	Coherence	PSD outside B1	PSD in MC	PSD Ratio (Test/Reference)
5.3	Continuous (Daytime) Periodic (Nighttime)	SR Chiller	0.20	$5.66 * 10^{-9}$	$4.46 * 10^{-9}$	1.3
9.0	Continuous (Daytime)	B1 Chiller	0.20	$3.86 * 10^{-9}$	$1.89 * 10^{-9}$	2.0
9.4	Continuous (Daytime)	B1 Chiller	0.26	$3.07 * 10^{-9}$	$1.51 * 10^{-9}$	2.0
15.6	Continuous (Daytime)	B1 Chiller	0.41	$2.51 * 10^{-9}$	$5.69 * 10^{-10}$	4.4
21.8	Continuous (Daytime)	B1 Chiller	0.43	$1.08 * 10^{-9}$	$5.07 * 10^{-10}$	2.1
48.9	Continuous (Daytime)	B1 Chiller	0.41	$3.60 * 10^{-10}$	$1.55 * 10^{-10}$	2.3
58.7	Continuous (Daytime) Periodic (Nighttime)	SR Chiller	Negligible	$3.04 * 10^{-10}$	$4.53 * 10^{-10}$	0.21
87.3	Continuous (Daytime)	B1 Chiller	Negligible	$8.52 * 10^{-10}$	$3.30 * 10^{-10}$	2.6

TABLE V: Noise lines found in coherence between seismometers outside of B1 and the MC. Note: For 48.9Hz, these values were calculated during a time that the MC's cold water chiller was seen to be off, for otherwise that source dominated this line.

Frequency (Hz)	Periodicity (Period)	Suspected Source	Coherence	PSD outside MC	PSD in MC	PSD Ratio (Test/Reference)
24.2	Continuous	MC Chiller	0.22	$2.45 * 10^{-9}$	$1.20 * 10^{-9}$	2.0
38.8	Continuous	MC Chiller	0.14	$2.83 * 10^{-9}$	$1.58 * 10^{-9}$	1.7
48.9, 97.8	Periodic (21.5 Minutes)	MC Chiller	0.21	$1.09 * 10^{-7}$	$5.10 * 10^{-10}$	220

TABLE VI: Noise lines found in coherence between seismometers outside of the MC and in the MC.

Frequency (Hz)	Periodicity (Period)	Suspected Source	Coherence	PSD near WEB	PSD in WEB	PSD Ratio (Test/Reference)
7.05	Continuous	Unknown	0.38	$3.23 * 10^{-9}$	$2.50 * 10^{-9}$	1.3
24.7	Continuous	Unknown	0.25	$1.44 * 10^{-9}$	$9.06 * 10^{-10}$	1.6
47.1	Continuous	Warm Water Pump	0.32	$1.82 * 10^{-9}$	$1.67 * 10^{-9}$	1.1
48.8	Continuous	Cold Water Pump	0.41	$2.50 * 10^{-9}$	$4.13 * 10^{-10}$	6.1
53.1	Continuous	HVAC	0.48	$8.97 * 10^{-10}$	$7.80 * 10^{-10}$	1.1
60.1	Continuous	HVAC	0.34	$7.82 * 10^{-10}$	$3.86 * 10^{-10}$	2.0
70.9	Continuous	Unknown	0.34	$1.95 * 10^{-9}$	$3.33 * 10^{-10}$	5.9
77.8	Continuous	Unknown	0.40	$2.20 * 10^{-9}$	$4.37 * 10^{-10}$	5.0

TABLE VII: Noise lines found in coherence between the WEB machinery and the WEB test mass. The HVAC lines were identified during a switch-off test after VSR2.

APPENDIX B: NOISE LINE TABLES

Frequency (Hz)	Periodicity (Period)	Suspected Source	Coherence	PSD near NEB	PSD in NEB	PSD Ratio (Test/Reference)
13.7	Continuous	Unknown	0.36	$2.20 * 10^{-9}$	$1.07 * 10^{-9}$	2.1
20.9	Continuous	HVAC	0.46	$2.73 * 10^{-9}$	$2.23 * 10^{-9}$	1.2
22.8	Continuous	Water Pump	0.32	$2.11 * 10^{-9}$	$4.99 * 10^{-10}$	4.2
23.7	Continuous	HVAC	0.52	$7.53 * 10^{-9}$	$1.78 * 10^{-9}$	4.2
48.7,97.4	Continuous	Water Pump	0.36	$3.96 * 10^{-9}$	$1.54 * 10^{-9}$	2.6
56.9	Continuous	HVAC	0.47	$1.03 * 10^{-8}$	$6.02 * 10^{-10}$	17

TABLE VIII: Noise lines found in coherence between the NEB machinery and the NEB test mass. The HVAC lines were identified during a switch-off test after VSR2.

APPENDIX C: PSD PLOTS

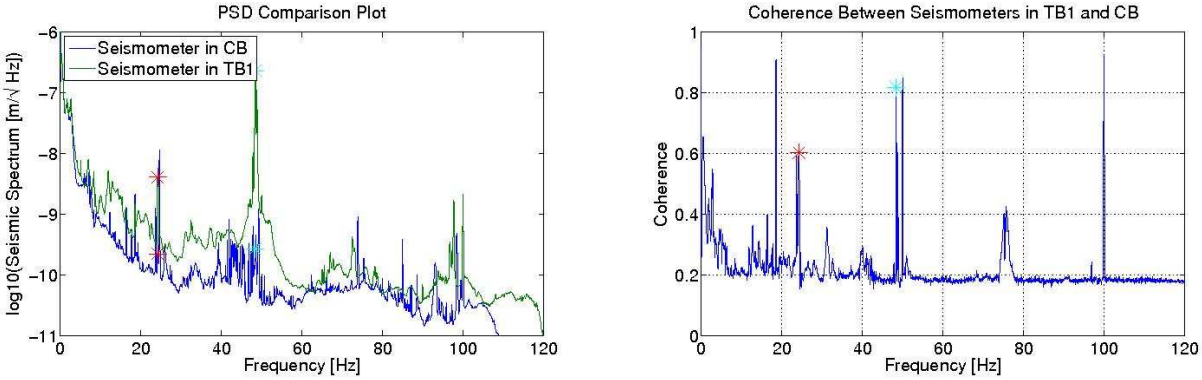

FIG. 22: Left: PSDs of the seismometers in TB1 and the CB. The peaks topped by red stars correspond to the 24.2Hz periodic line while the blue stars correspond to the 48Hz continuous line. Right: Coherence between seismometers in TB1 and the CB. The peak topped by the red star corresponds to the 24.2Hz periodic line while the blue star corresponds to the 47.9Hz continuous line.

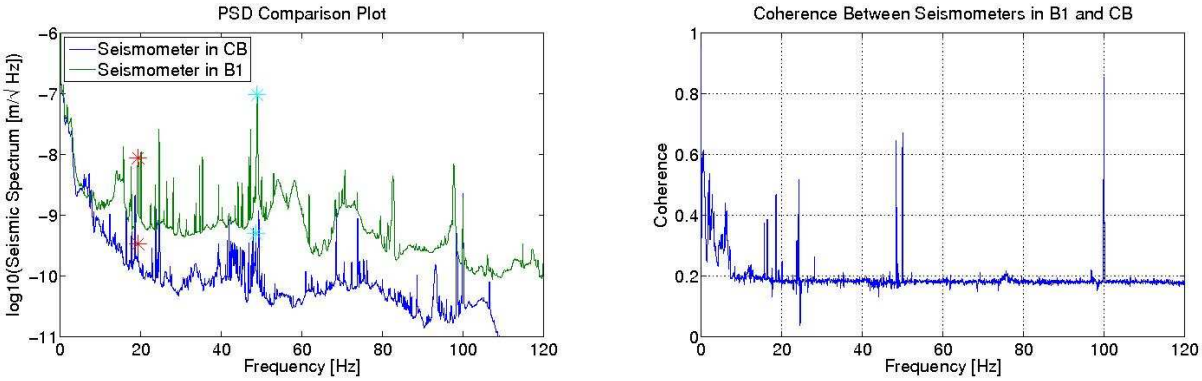

FIG. 23: Left: PSDs of the seismometers in B1 and the CB. The red stars on the left correspond to the 19.3Hz line while the blue stars on the right correspond to the 48.4Hz line. Right: Coherence between seismometers in B1 and the CB.

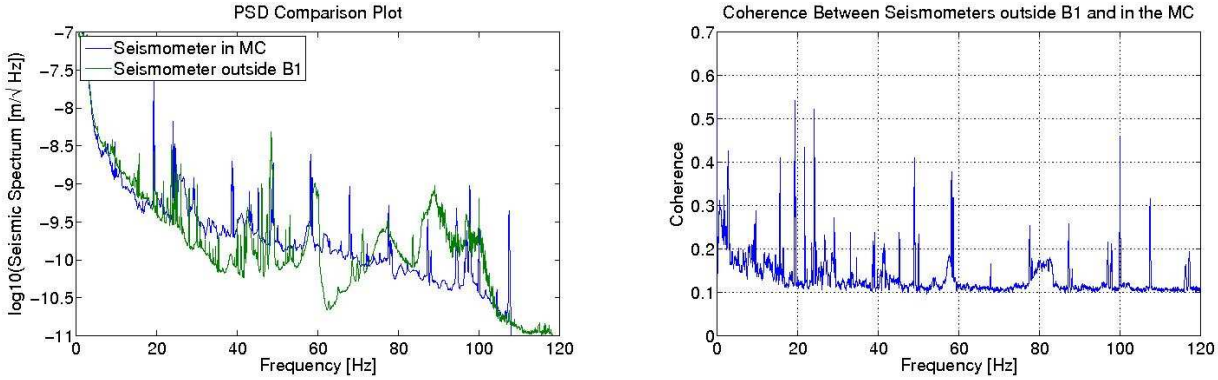

FIG. 24: Left: PSDs of the seismometers outside B1 and in the MC. Right: Coherence between seismometers outside B1 and in the MC.

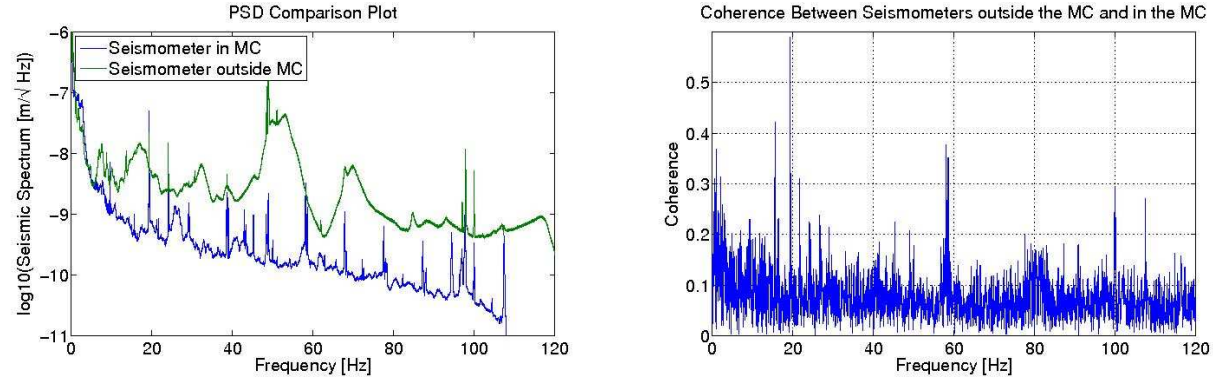

FIG. 25: Left: PSDs of the seismometers outside the MC and in the MC. Right: Coherence between seismometers outside the MC and in the MC. This plot was computed with a 60 second offset and it seems that the test probe's proximity to the chiller has made an accurate coherence estimate difficult.

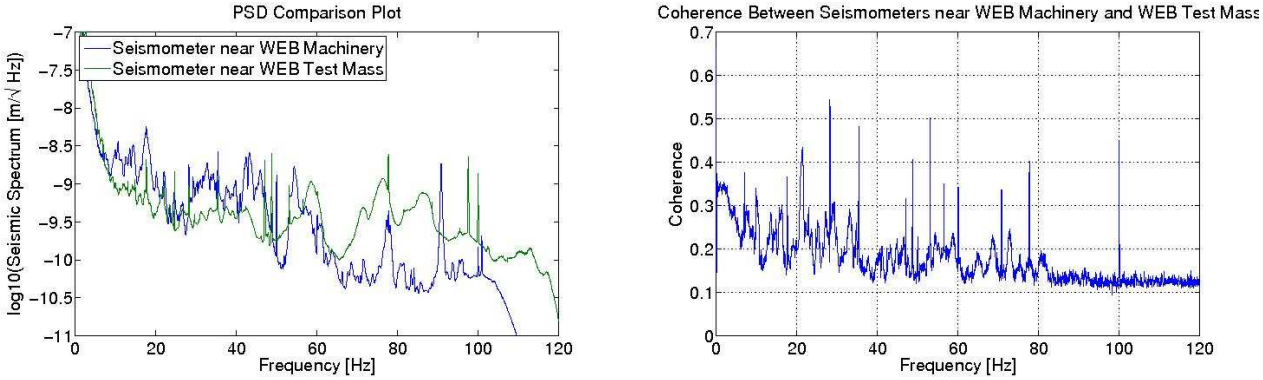

FIG. 26: Left: PSDs of the seismometers near the WEB machinery and near the WEB test mass. Right: Coherence between the seismometers near the WEB machinery and near the WEB test mass.

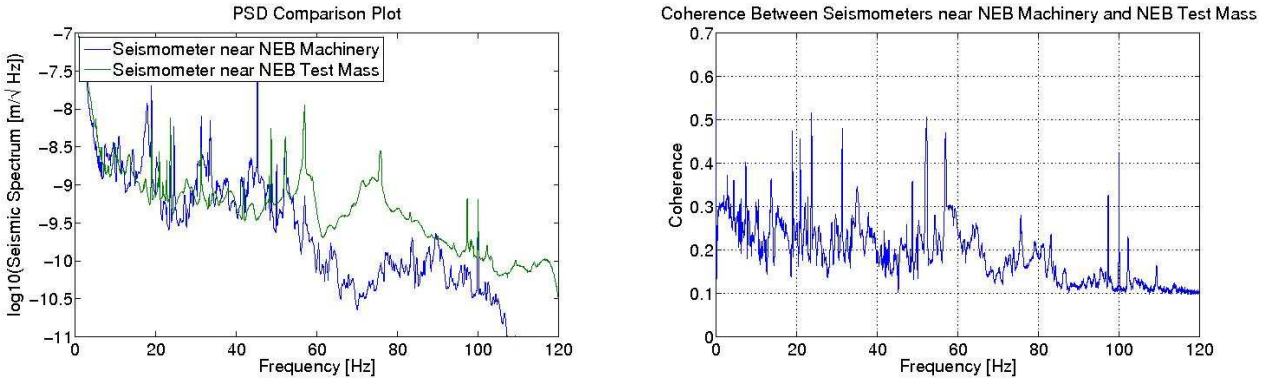

FIG. 27: Left: PSDs for the seismometers near the NEB machinery and near the NEB test mass. Right: Coherence between the seismometers near the NEB machinery and near the NEB test mass.